

Quantification of Oxygen and Carbon in Calcium Targets for Reliable $\text{Ca}(p, p\alpha)$ Measurements

Junki Tanaka^{1,2,*}, Riku Matsumura^{3,4}, and Taichi Miyagawa^{1,2}
for the ONOKORO collaboration

¹Research Center for Nuclear Physics (RCNP), The University of Osaka, Osaka 567-0047, Japan

²Department of Physics, The University of Osaka, Osaka 560-0043, Japan

³Graduate School of Science and Engineering, Saitama University, Saitama 338-8570, Japan

⁴RIKEN Nishina Center for Accelerator-Based Science, Saitama 351-0198, Japan

Abstract. Reliable extraction of $\text{Ca}(p, p\alpha)$ cross sections requires accurate correction for oxygen and carbon impurities in calcium targets. In this work, the relative amounts of these light elements in $^{40,42,44,48}\text{Ca}$ targets are determined using 65-MeV proton elastic scattering, where the Ca/Mylar yield ratios provide a direct measure of the corresponding O and C atomic ratios. These experimentally determined ratios are then applied to the 392-MeV $(p, p\alpha)$ spectra to subtract the O and C contributions in a fully data-driven manner. The method does not rely on assumptions about absolute contamination levels or reaction-model calculations, and enables a consistent and reliable determination of $\text{Ca}(p, p\alpha)$ yields across the calcium isotopic chain.

The α -knockout method has become a powerful probe of cluster correlations in the nuclear surface region [1], where the reduced nuclear density is expected to enhance the emergence of cluster degrees of freedom. This approach can be extended to a wide range of nuclei and reaction channels, including t , ^3He , and d knockout, with the aim of establishing a unified description of cluster degrees of freedom in medium- to heavy-mass systems [2, 3].

A practical experimental challenge in $\text{Ca}(p, p\alpha)$ measurements is the presence of small oxygen and carbon impurities introduced during target preparation. Although their absolute concentrations are low, the corresponding $\text{O}(p, p\alpha)$ and $\text{C}(p, p\alpha)$ cross sections are significantly larger than those of Ca, reflecting the lighter masses and more weakly bound cluster structures of these nuclei. In addition, their α -separation energies (S_α) are close to those of the Ca isotopes. As a consequence, $\text{O}/\text{C}(p, p\alpha)$ events appear in the same S_α region as the $\text{Ca}(p, p\alpha)$ signals and cannot be distinguished by kinematic selection alone. A quantitative evaluation of these contributions is therefore essential for reliable isotopic comparisons.

Table 1 summarizes the thicknesses, isotope enrichment, and α -separation energies of the Ca targets used in the present study.

In the present work, the relative amounts of ^{16}O and ^{12}C in the Ca isotopic targets are determined using 65-MeV proton elastic-scattering measurements. These measurements were performed under identical experimental conditions for the Ca isotopes and the Mylar reference target, allowing a direct comparison of elastic-scattering yields.

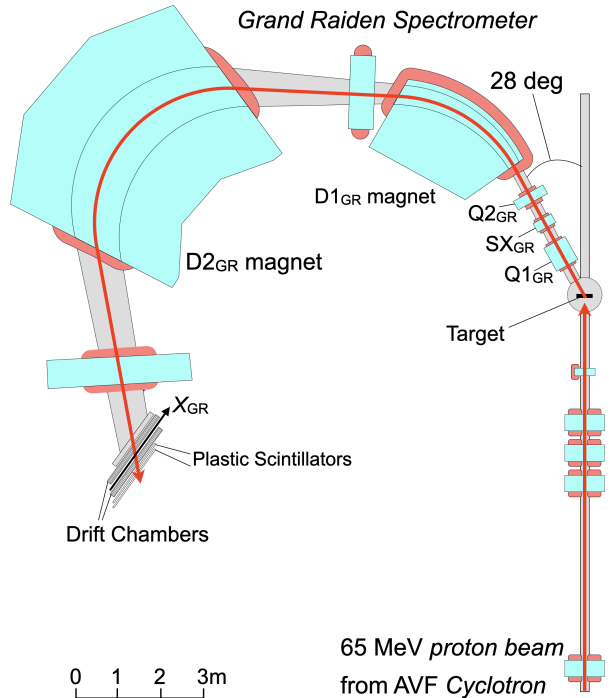


Figure 1: The Grand Raiden spectrometer was positioned at a laboratory angle of $\theta_{\text{lab}} = 28^\circ$ with respect to the beam axis. Elastically scattered protons were transported to the focal plane and measured using drift chambers for position determination and plastic scintillators for energy-loss and timing measurements. Identical spectrometer settings were employed for the Ca and Mylar targets to ensure identical kinematic and acceptance conditions.

*e-mail: junki@rcnp.osaka-u.ac.jp

Target Isotope	Thickness (mg/cm ²)	Enrichment (%)	S_α (MeV)
⁴⁰ (nat)Ca	11.8 (1.1)	96.9	7.039
⁴² Ca	10.0 (1.0)	91.2	6.257
⁴⁴ Ca	9.7 (1.0)	88.5	8.854
⁴⁸ Ca	10.0 (1.0)	97.8	13.977

Table 1: Thicknesses, isotope enrichment, and α -separation energies of the Ca targets used in this work.

The essential point of this approach is that the ratio of the $^{16}\text{O}(p, p)$ elastic-scattering yields per unit luminosity between the Ca and Mylar targets depends solely on the relative number of oxygen atoms and is independent of the reaction mechanism and absolute cross sections. The same procedure is applied to ^{12}C . These experimentally determined ratios are directly used in the subsequent 392-MeV ($p, p\alpha$) analysis to quantify and subtract the O/C contributions in the Ca spectra, without relying on assumptions about absolute contamination levels. This strategy provides a consistent and robust correction procedure for extracting reliable Ca($p, p\alpha$) yields across the calcium isotopic chain. In the present work, the relative amounts of ^{16}O and ^{12}C in the Ca isotopic targets are determined using 65-MeV proton elastic-scattering measurements performed under identical experimental conditions for the Ca and Mylar targets. Under these identical kinematic and instrumental conditions, the ratio of the $^{16}\text{O}(p, p)$ elastic-scattering yields per unit luminosity between the two targets depends only on the relative number of oxygen atoms and is therefore independent of the reaction mechanism and absolute cross sections. These experimentally determined ratios are directly applied to the 392-MeV ($p, p\alpha$) analysis to quantify the O/C contributions in the Ca spectra, without relying on absolute contamination levels. This strategy ensures a consistent and robust correction procedure for extracting reliable Ca($p, p\alpha$) yields across the Ca isotopic chain. Elastic-scattering measurements were carried out at RCNP using a 65-MeV proton beam accelerated by the AVF cyclotron. The Grand Raiden spectrometer [4] was set at a laboratory angle of $\theta_{\text{lab}} = 28^\circ$, and its magnetic fields were optimized for the detection of elastically scattered protons. Data were collected for ⁴⁰(nat)Ca, ⁴²Ca, ⁴⁴Ca, ⁴⁸Ca, and Mylar targets under identical experimental conditions, enabling a direct and consistent comparison of the O(p, p) and C(p, p) yields. The energy acceptance of approximately 10% allowed elastically scattered protons from all target nuclei to be detected within a single spectrometer setting. To ensure comparable energy resolution between the Ca and Mylar measurements, the Mylar foil thickness was chosen such that the resulting energy straggling was essentially identical to that of the Ca targets. As a result, the energy resolution of the 65-MeV elastic-scattering spectra was nearly identical for all targets, with a typical value of FWHM ≈ 50 keV, primarily determined by the energy spread of the incident beam.

Figure 2 shows the resulting spectra. The lower horizontal axis represents the X position at the focal plane of the Grand Raiden spectrometer, which is converted to the

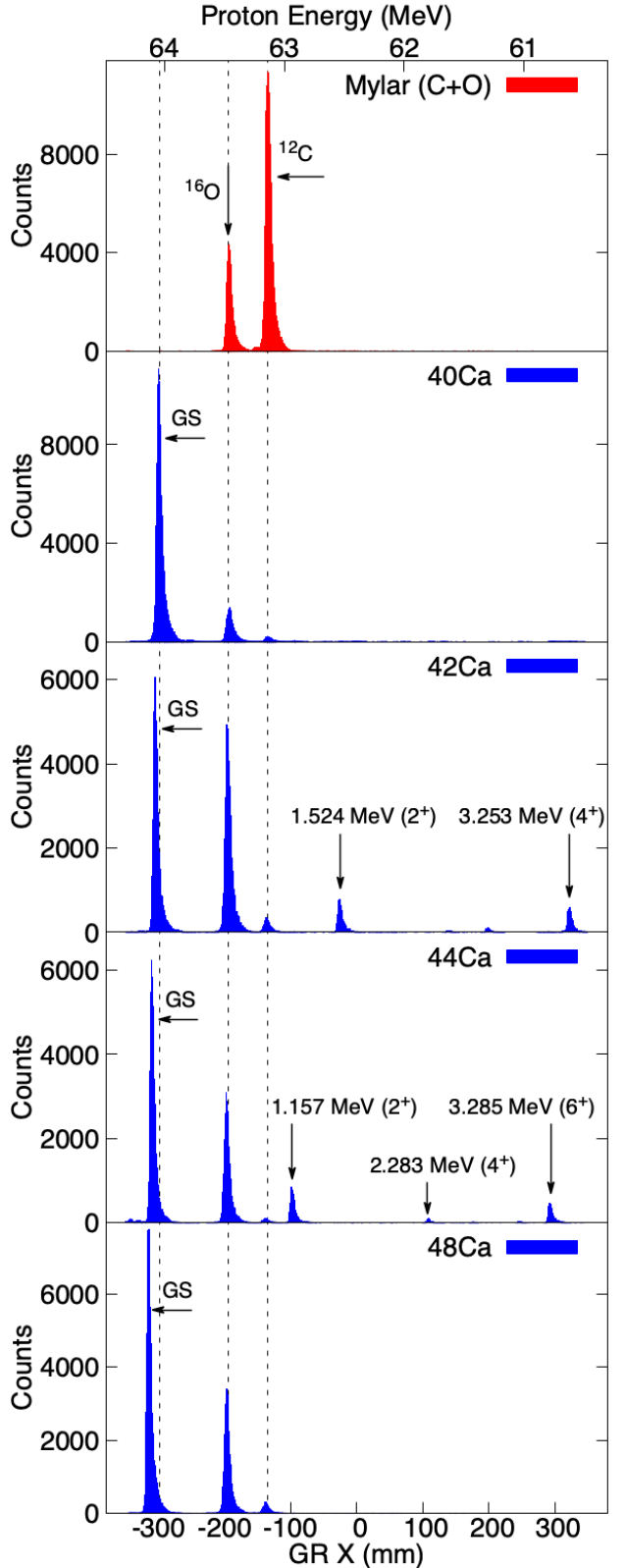


Figure 2: Grand Raiden focal-plane X position distributions corresponding to the energy spectra of protons from 65-MeV elastic scattering on the Mylar, ^{nat}Ca, ⁴²Ca, ⁴⁴Ca, and ⁴⁸Ca targets.

proton energy on the upper axis. In the Mylar spectrum (top), prominent peaks originating from elastic scattering on ^{16}O and ^{12}C are observed. The ^{40}Ca spectrum (sec-

ond) exhibits a dominant elastic ground-state (GS) peak, accompanied by smaller contributions from ^{16}O and ^{12}C . The spectra for ^{42}Ca (third) and ^{44}Ca (fourth) show, in addition to the ground state, several inelastic peaks that are assigned to known excited states based on their energies. For ^{48}Ca (bottom), the first 2^+ state lies outside the present energy acceptance, and only the ground-state peak is observed. A systematic shift of the Ca elastic peaks reflects the change in isotope mass and confirms both the isotope selection and the high isotopic purity of the targets. In all spectra, the ^{16}O and ^{12}C peaks appear at identical energies, as indicated by the dotted reference lines.

The oxygen content in each target is determined from the $^{16}\text{O}(p, p)$ yields $Y_{^{16}\text{O}(p,p)}$, which are related to the elastic differential cross section ($d\sigma/d\Omega_{\text{el}}$) by

$$Y_{^{16}\text{O}(p,p)}^{(\text{Ca})} = \left(\frac{d\sigma}{d\Omega} \right)_{\text{el}} Q^{(\text{Ca})} N_{^{16}\text{O}}^{(\text{Ca})} \Delta\Omega, \quad (1)$$

$$Y_{^{16}\text{O}(p,p)}^{(\text{My})} = \left(\frac{d\sigma}{d\Omega} \right)_{\text{el}} Q^{(\text{My})} N_{^{16}\text{O}}^{(\text{My})} \Delta\Omega. \quad (2)$$

Here, Q is the accumulated beam charge measured during the experiment, N denotes the number of ^{16}O atoms in each target, and $\Delta\Omega$ is the solid angle of the spectrometer.

Because the Ca and Mylar targets were measured under identical kinematic and instrumental conditions, taking the yield ratio eliminates the dependence on the absolute cross section and the solid angle:

$$\frac{N_{^{16}\text{O}}^{(\text{Ca})}}{N_{^{16}\text{O}}^{(\text{My})}} = \frac{Y_{^{16}\text{O}(p,p)}^{(\text{Ca})}}{Y_{^{16}\text{O}(p,p)}^{(\text{My})}} \cdot \frac{Q^{(\text{My})}}{Q^{(\text{Ca})}}. \quad (3)$$

This ratio depends solely on the relative number of oxygen atoms in the two targets. This reaction-independent property provides the basis for applying the 65-MeV normalization factors directly to the 392-MeV ($p, p\alpha$) analysis. Table 2 summarizes the measured $^{16}\text{O}(p, p)$ yields, the effective beam charges, and the resulting oxygen ratios. The same procedure is applied to ^{12}C , whose contamination level is determined using an identical ratio formulation.

With the number ratios of ^{16}O and ^{12}C relative to the Mylar target established at 65 MeV, their contributions to the 392-MeV ($p, p\alpha$) spectra are evaluated. A 65-MeV proton beam from the AVF cyclotron was subsequently accelerated to 392 MeV by the Ring Cyclotron. Using a double-arm spectrometer operated under identical settings, ($p, p\alpha$) reactions were measured for the Ca isotopes, Mylar, and an additional ^{nat}C target. Protons were detected with the Grand Raiden spectrometer at 45° , and α particles with the Large Acceptance Spectrometer (LAS) at 58° , corresponding to quasi-free kinematic conditions.

For each target, α -separation-energy S_α spectra were constructed using the missing-mass method and normalized by the accumulated beam charge. Details of the analysis procedure are described in Ref. [1].

The yields of the $^{16}\text{O}(p, p\alpha)$ S_α spectra for the Ca and Mylar targets are expressed as

$$\frac{Y_{^{16}\text{O}(p,p\alpha)}^{(\text{Ca})}}{Q^{(\text{Ca})}} = \left(\frac{d^3\sigma}{d\Omega_p d\Omega_\alpha dS_\alpha} \right)_{^{16}\text{O}(p,p\alpha)} N_{^{16}\text{O}}^{(\text{Ca})} \Delta\Omega_p \Delta\Omega_\alpha \Delta S_\alpha, \quad (4)$$

$$\frac{Y_{^{16}\text{O}(p,p\alpha)}^{(\text{My})}}{Q^{(\text{My})}} = \left(\frac{d^3\sigma}{d\Omega_p d\Omega_\alpha dS_\alpha} \right)_{^{16}\text{O}(p,p\alpha)} N_{^{16}\text{O}}^{(\text{My})} \Delta\Omega_p \Delta\Omega_\alpha \Delta S_\alpha, \quad (5)$$

where $\Delta\Omega_p$ and $\Delta\Omega_\alpha$ denote the solid-angle acceptances of the proton and α spectrometers, respectively, and ΔS_α is the bin width of the S_α spectrum.

The reaction kinematics is uniquely determined once the proton scattering angle Ω_p , the α emission angle Ω_α , and one additional kinematic variable are specified. In the present analysis, the α -separation energy S_α , reconstructed using the missing-mass method, is chosen as this third variable. With this choice, each $(\Omega_p, \Omega_\alpha, S_\alpha)$ bin corresponds to a unique reaction kinematics, and the yield in that bin is proportional to the triple-differential cross section.

The triple-differential cross section $(d^3\sigma/d\Omega_p d\Omega_\alpha dS_\alpha)_{^{16}\text{O}(p,p\alpha)}$ depends only on the $^{16}\text{O}(p, p\alpha)$ reaction mechanism and kinematics. Because the Ca and Mylar measurements were performed with the same incident beam energy, spectrometer settings, and angular acceptances, the reaction conditions for ^{16}O are identical in both targets. Consequently, the triple-differential cross section is common to Eqs. 4 and 5.

Equation 4 represents the $^{16}\text{O}(p, p\alpha)$ yield arising from the ^{16}O impurities in the Ca target. Because this contribution appears at the same S_α values as the $\text{Ca}(p, p\alpha)$ reaction, it overlaps with the Ca spectrum and cannot be isolated from the Ca-target data alone.

Equation 5 gives the $^{16}\text{O}(p, p\alpha)$ yield obtained from the Mylar target. In the Mylar data, the ^{16}O and ^{12}C contributions can be separated, since the $^{12}\text{C}(p, p\alpha)$ spectrum is independently determined. Subtracting this known ^{12}C contribution therefore provides a reference $^{16}\text{O}(p, p\alpha)$ spectrum free of Ca-related components.

Taking the ratio of Eqs. 4 and 5 cancels the spectrometer acceptances $\Delta\Omega_p \Delta\Omega_\alpha$, the S_α bin width ΔS_α , and the absolute $^{16}\text{O}(p, p\alpha)$ triple-differential cross section. The resulting relation depends only on the relative number of ^{16}O atoms in the two targets:

$$\frac{Y_{^{16}\text{O}(p,p\alpha)}^{(^{40}\text{Ca})}}{Q^{(^{40}\text{Ca})}} = \left(\frac{N_{^{16}\text{O}}^{(^{40}\text{Ca})}}{N_{^{16}\text{O}}^{(^{40}\text{Ca})}} \right) \frac{Y_{^{16}\text{O}(p,p\alpha)}^{(\text{My})}}{Q^{(\text{My})}}, \quad (6)$$

$$\frac{Y_{^{16}\text{O}(p,p\alpha)}^{(^{44}\text{Ca})}}{Q^{(^{44}\text{Ca})}} = \left(\frac{N_{^{16}\text{O}}^{(^{44}\text{Ca})}}{N_{^{16}\text{O}}^{(^{44}\text{Ca})}} \right) \frac{Y_{^{16}\text{O}(p,p\alpha)}^{(\text{My})}}{Q^{(\text{My})}}. \quad (7)$$

Figures 4 and 3 show the measured ($p, p\alpha$) S_α spectra for ^{40}Ca and ^{44}Ca , respectively, together with the estimated oxygen and carbon contributions obtained using the procedure described above. The yield is normalized per incident proton, where the measured beam charge Q is converted to the number of incident particles N via $Q = eN$.

Table 2: Summary of $^{16}\text{O}/^{12}\text{C}(p, p)$ yields, beam charges, and the ratios to the Mylar target.

Target	$Y_{^{16}\text{O}(p,p)}$	$Y_{^{12}\text{C}(p,p)}$	Q (nC)	$N_{^{16}\text{O}}^{(\text{Target})}/N_{^{16}\text{O}}^{(\text{My})}$	$N_{^{12}\text{C}}^{(\text{Target})}/N_{^{12}\text{C}}^{(\text{My})}$
Mylar	547026	1286616	7148	1.0000 (0.0026)	1.0000 (0.0021)
^{40}Ca	211571	30235	29277	0.0944 (0.0003)	0.0057 (0.0001)
^{42}Ca	645655	44770	18626	0.4530 (0.0011)	0.0134 (0.0001)
^{44}Ca	357845	13657	16477	0.2838 (0.0008)	0.0046 (0.0001)
^{48}Ca	410519	38687	16103	0.3331 (0.0009)	0.0133 (0.0001)

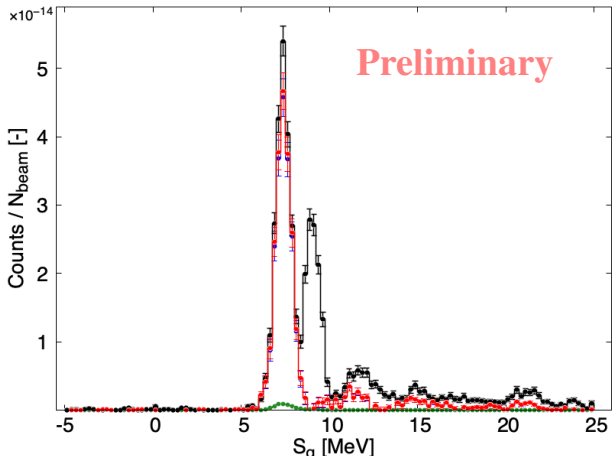


Figure 3: $(p, p\alpha)$ S_α spectrum for the ^{44}Ca target. The black curve shows the measured spectrum. The blue and green curves indicate the estimated $^{16}\text{O}(p, p\alpha)$ and $^{12}\text{C}(p, p\alpha)$ contributions, respectively, scaled from the Mylar reference data. The red curve represents their sum.

As shown in Fig. 3, for the ^{44}Ca target the $\text{O}(p, p\alpha)$ and $\text{C}(p, p\alpha)$ components are distributed around $S_\alpha \simeq 7$ MeV, while the $^{44}\text{Ca}(p, p\alpha)^{40}\text{Ar}$ peak is located near $S_\alpha \simeq 9$ MeV. The separation between these components is about 2 MeV in S_α . Under this condition, the summed O/C contribution scaled from the Mylar reference is overlaid on the Ca-target spectrum without additional normalization. The difference between the O/C yields extracted from the Ca-target data and those estimated from the Mylar reference provides an estimate of the associated systematic uncertainty. Benchmarking this procedure against independent data sets yields a reproducibility of 7%.

In contrast, Fig. 4 shows that for ^{40}Ca the $^{40}\text{Ca}(p, p\alpha)^{36}\text{Ar}$ peak is located in the same S_α region as the oxygen and carbon contributions, around $S_\alpha \simeq 7$ MeV. In this region, the estimated O/C contribution amounts to approximately 25% of the total yield. Propagating the 7% uncertainty of the O/C estimation therefore results in a systematic uncertainty of $0.25 \times 0.07 \simeq 0.02$, corresponding to a 2% uncertainty in the extracted $^{40}\text{Ca}(p, p\alpha)$ yield. This contribution is smaller than other dominant systematic uncertainty, such as those arising from the target thickness.

Overall, the consistency between the Ca-target data and the Mylar-scaled O/C contributions, quantified by the

reproducibility of the extracted yields, supports the validity of the data-driven procedure used to quantify oxygen and carbon impurities. Because the method relies exclusively on experimentally determined yield ratios, it does not require assumptions on absolute contamination levels or reaction models. The resulting uncertainty satisfies the precision requirements of the present analysis and is consistently applied across the calcium isotopic chain.

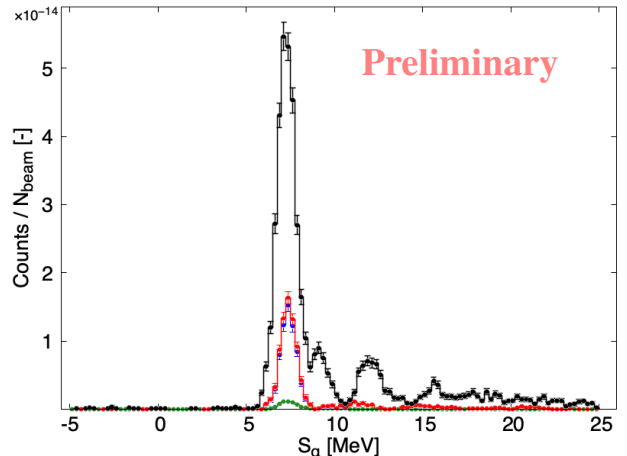


Figure 4: $(p, p\alpha)$ S_α spectrum for the ^{40}Ca target. The black curve shows the measured spectrum. The blue and green curves indicate the estimated $^{16}\text{O}(p, p\alpha)$ and $^{12}\text{C}(p, p\alpha)$ contributions, respectively, scaled from the Mylar reference data. The red curve represents their sum.

Acknowledgments The authors thank the accelerator group at RCNP for their technical support. This work was supported by JSPS KAKENHI (JP21H04975) and the JSPS A3 Foresight Program “Nuclear Physics in the 21st Century.” Additional support was provided by the NRF TOPTIER Korea–Japan Joint Research Program (RS-2024-00436392), IBS (IBS-R031-D1) in Korea, and the National Key R&D Program of China (2023YFE0101500).

References

- [1] J. Tanaka, Z. Yang, *et al.*, *Science* **371**, 260 (2021).
- [2] T. Uesaka and N. Itagaki, *Philos. Trans. R. Soc. A* **382**, 20230123 (2024).
- [3] Y. Kubota, *et al.*, *Nucl. Phys. A* **1060**, 123123 (2025).
- [4] M. Fujiwara, *et al.*, *Nucl. Instrum. Methods Phys. Res. A* **422**, 484 (1999).